Chapter 11
Advanced Corrosion Prevention Approaches: Smart Coating and Photoelectrochemical Cathodic Protection

Viswanathan S. Saji

11.1 Introduction

Corrosion is a natural process causing materials damage and components failures. The worldwide corrosion cost is projected to be approximately US$ 2.5 trillion, which is equivalent to 3.4% of the global gross domestic product (GDP) [1–3]. Appropriate modifications in the material (e.g. corrosion-resistant alloys), environment (e.g. corrosion inhibitors) or material's surface (e.g. coatings) is requisite for effective corrosion protection. Corrosion can also be prevented by cathodic (by sacrificial anode or impressed current methods) and anodic methods [4, 5]. In several industrial applications, a combination of surface coatings and cathodic protection (CP) can deliver the most effective corrosion mitigation. Coatings alone may not be fully adequate to provide corrosion protection for the underlying metal in aggressive environments such as seawater as they are accompanied by microscopic pores, and the coating defects increase with the increase in service time. Conversely, CP alone is generally not cost-effective.

Seawater desalination has emerged as a viable alternative water supply in the modern world, predominantly in arid countries. Research and development over the last five decade in this area bring about many advancements leading to more efficient and cost-effective desalination systems [6, 7]. However, corrosion remains a major threat in seawater desalination systems. The average salinity of seawater is ~ 3.5%, and the oxygen concentration reaches a maximum at this salt level. Combined with the high oxygen and the salt content and the presence of various other aggressive species, microbes, fouling agents and pollutants make seawater extremely corrosive to structural materials.

V. S. Saji (✉)
King Fahd University of Petroleum and Minerals, Center of Research Excellence in Corrosion, Dhahran 31261, Saudi Arabia
e-mail: saji.viswanathan@kfupm.edu.sa

V. S. Saji et al. (eds.), *Corrosion and Fouling Control in Desalination Industry*,
https://doi.org/10.1007/978-3-030-34284-5_11

The primary objective of this chapter is to provide a concise description of two selected cutting-edge corrosion control approaches, one each from the surface coating and the CP, which can be employed in desalination industries for more effective corrosion protection. The first section of the chapter deals with smart coatings, an attractive coating approach that can deliver controlled active protection with self-healing abilities. The smart coating approaches are explained with reference to supramolecular interactions. The second section explains impending solar energy assisted CP method; namely photoelectrochemical cathodic protection (PECP).

11.2 Smart Coatings

A corrosion protective surface coatings in general works by passive protection or active protection. The passive protection depends entirely on the coating's barrier properties, whereas the active protection depends on the incorporated corrosion inhibitors in the coating matrix [8–10]. The smart coating concept makes use of both the active and the passive protection intelligently via the controlled on-demand release of inhibitors.

In general, a smart coating approach relies on a specialized resin, pigment, or other material that can respond to an environmental stimulus and react to it. Instead of direct doping of corrosion inhibitors in the coating matrix, a smart coating utilizes approaches such as encapsulation of inhibitors in nano/microcontainers that are dispersed homogeneously in the host coating [11, 12]. The immobilization/encapsulation method can overcome the problems with the direct doping approach, such as early inhibitor leakage and undesirable inhibitor-matrix interactions [13]. When the coating is damaged, the incorporated containers releases the pre-loaded inhibitors to repair the defects. A perfect nano/microcontainer is projected to be featured with the following attributes [14]:

(i) Chemical and mechanical stability
(ii) Compatibility with the coating matrix
(iii) Adequate loading capability
(iv) An impervious covering wall to avoid leakage of the active matter
(v) Skill to sense corrosion initiation
(vi) Release of the active matter on response.

The smart coating relies on supramolecular chemical approaches [15]. Supramolecular chemistry, otherwise called 'chemistry of molecular assemblies' or 'the chemistry of the intermolecular (non-covalent) bond', are branded by the three-dimensionally arranged supramolecular species with intermolecular interactions (e.g., ion-ion, ion-dipole, dipole-dipole, hydrogen bonding, π–π, etc.). Supramolecular compounds can be conveniently categorized into (i) molecular self-assemblies, (ii) host-guest complexes, and (iii) molecules built to specific shapes (rotaxanes, dendrimers etc.). In the host-guest chemistry-based systems, a host (a large molecule, aggregate or a cyclic compound having a cavity) binds a guest

molecule making a host-guest supramolecule. More details on supramolecular compounds can be found elsewhere [15–20].

Structural alterations of supramolecular assemblies permit stimuli responsiveness. The nanocontainers disseminated in coatings can discharge the captured inhibitors in a regulated manner, which can be accustomed to occur along with the corrosion instigation or local environment changes (temperature, pH or pressure changes, radiation, mechanical action etc.) by using reversible covalent bonds or feebler non-covalent interactions. Smart coatings can be divided into several types based on the functionalization, and that can have several functions such as self-cleaning, self-healing, anti-biofouling and anti-corrosion [12, 21–29]. Several research efforts are presently ongoing in fabricating porous, hollow, or layer structured nanocontainers. Here, we describe recent research advancements in nano/microcontainers where supramolecular approaches are utilized in crafting more proficient smart coatings.

11.2.1 Polymer-Based Nano/Microcapsules

Polymeric capsules have been explored extensively as a carrier of core components in smart coating applications. Here, the active constituent (core) is embedded within another material (shell) to protect the core from the direct surroundings. Either monomers/pre-polymers (by methods such as emulsion polymerization, interfacial polycondensation etc.) or polymers (by suspension cross-linking, solvent extraction etc.) can be employed for the production of nano/microcontainers. Polyurea (PUA)-formaldehyde and polyurethane (PU)-based containers were among the first strategies developed in this area [30].

Huang et al. prepared PU microcapsules encircling hexamethylene diisocyanate via interfacial polymerization of methylene diphenyl diisocyanate prepolymer and 1,4-butanediol in oil-in-water emulsion [31]. Latnikova et al. showed that the type of polymer used had a noteworthy influence on the structure of the capsules formed. The PU and PUA loaded with the inhibitors were found to be evenly dispersed in the polymer matrix when compared with polyamide containers [32]. Gite et al. on their studies on quinoline incorporated PUA microcapsules showed that well defined, thermally stable spherical microcapsules with mean diameters of 72 and 86 μm were displayed excellent thermal and storage stabilities up to 200 °C [33]. All these studies presented considerably enhanced corrosion resistance for the self-healing coating after incorporating an optimized amount of microcapsules. For example, a low corrosion rate of 0.65 mm year^{-1} was obtained in 5 wt.% HCl for mild steel coated with PU with the incorporation of 4 wt.% of microcapsules loaded quinoline corrosion inhibitor [33]. Li et al. described pH-responsive polystyrene (PS) nanocontainer where benzotriazole (BTA) inhibitors were encapsulated in the PS matrix during polymerization, and that was followed by adsorption of a highly branched polyethylenimine as a controlled release system of BTA [34]. Maia et al. showed that incorporation of PUA microcontainers loaded with 2-mercaptobenzothiazole

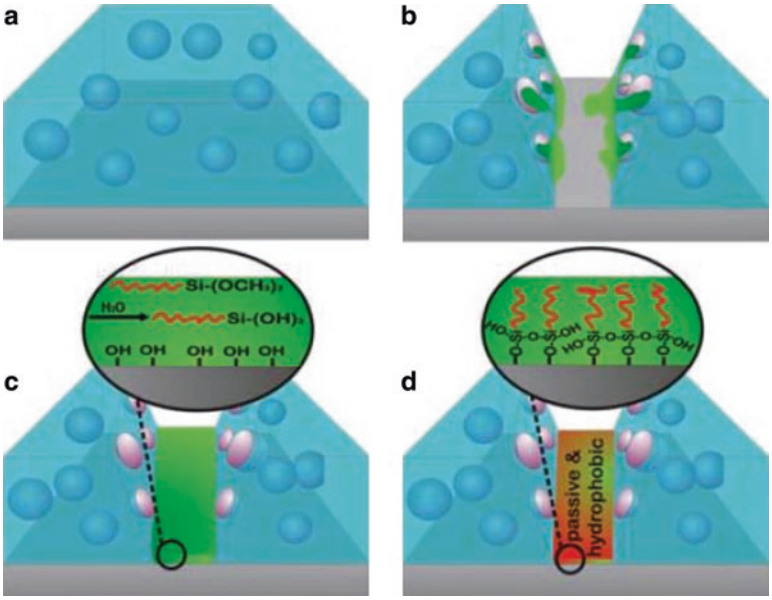

Fig. 11.1 Schematic of a self-healing smart coating. (**a**) Coating encompassing microcapsules loaded with alkoxysilanes on a metal substrate. (**b**) The release of encapsulated alkoxysilanes on coating damage. (**c**) The reaction of alkoxysilanes with H_2O from the ambient environment. (**d**) The damaged surface becomes passive and hydrophobic. Reproduced with permission from Ref. 36; Copyright 2011 © Royal Society of Chemistry

(MBT) in sol-gel coating (on 2024 Al alloy) was beneficial to improve the coating's barrier properties as well as coating adhesion [35]. Latnikova et al. described an intersting concept by the synergistic combination of the passivation and hydrophobicity (Fig. 11.1) where alkoxysilanes with long hydrophobic tails were captured in PU microcapsules. On coating damage, the released alkoxysilanes form covalent interaction with the hydroxyl groups on the metal surface developing an inactive electrochemical film. The highly hydrophobic properties ascribed to the long hydrocarbon tails enhanced the barrier properties by precluding water/aggressive ions infiltration [36]. Further details on polymeric nanocontainers can be found elsewhere [30]. Several studies investigated polymer nano/microgels-based novel carriers [37, 38].

11.2.2 Host-Guest Chemistry-Based

Stimulus feed-back anti-corrosion coatings, made-up by the dissemination of 'guest' materials (inhibitor loaded intelligent nanocontainers) into 'host' matrix have attracted considerable research attention [12, 26, 27, 39, 40]. The expected properties of the guest materials are:

(i) High loading capability
(ii) Good compatibility
(iii) Stimulus-responsiveness
(iv) Controlled release property
(v) Zero premature release
(vi) Prompt high sensitivity

Here, we provides a few examples of host-guest chemistry-based systems of mesoporous silica and cyclodextrins (CDs).

Mesoporous silica nanocontainers (MSNs) have attracted considerable research attention due to their large specific surface area, easy surface functionalization, biocompatibility, high stability, and controllable pore diameter [41–43]. Borisov et al. showed that too low concentrations (0.04 wt.%) of embedded nanocontainers led to good coating barrier properties, however, reduced active corrosion inhibition due to insufficient inhibitor availability. In contrast, higher concentrations of the nanocontainers (0.8–1.7 wt.%) degraded the coating integrity, leading to diffusion paths for aggressive species and reduced barrier effect. A coating with 0.7 wt.% inhibitor loaded MSNs exhibited the best corrosion protection [44, 45]. Zheludkevich et al. described a layer by layer (LBL) assembly where pH-sensitive silica nanoparticles were covered with polyelectrolyte layers, and layers of BTA and that was successively assimilated into a hybrid sol-gel coating (~ 95 mg of inhibitor /1 g of SiO_2). The enhancement of corrosion resistance was credited to the better adhesion, improved barrier effect, and placid inhibitor release. When corrosion commenced, the local pH changes and that opens the polyelectrolyte shell of the nanocontainers releasing BTA. After corrosion suppressed, the local pH gets recovered, closing the polyelectrolyte shell and terminating further inhibitor release [21]. Chen and Fu fabricated hollow mesoporous silica nanocontainers (diameter 0.5–08 μm, shell thickness ~ 100 nm) using poly(vinylpyrrolidone) and cetyltrimethylammonium bromide templates, and subsequently, pH-sensitive supramolecular nanovalves comprising of ucurbit [6] uril (CB [6]) rings and bisammonium stalks were anchored to the nanocontainers's outer surface. At neutral pH, the CB [6] incorporated the bisammonium stalks firmly, closing the nanopore orifices effectively, and once the pH augmented, the stalks became deprotonated and CB [6] de-threaded from the stalks, opening the nanovalves with inhibitor release [46, 47]. Ding et al. explored an innovative organic silane-based corrosion potential-stimulus feedback active coating (CP-SFAC) for Mg alloys, based on redox-responsive self-healing concept [48, 49] where the surface potential reduction after localized corrosion initiation was exploited as a trigger. The design utilized supramolecular self-assembly technique where corrosion potential-stimulus responsive nanocontainers (CP-SNCs) that were composed of Fe_3O_4@mSiO_2 as magnetic nanovehicles and bipyridinium ⊂ water-soluble pillar [5] arenes (BIPY ⊂ WP [5]) assemblies as gatekeepers/disulfide linkers. The Fe_3O_4@mSiO_2 produced by the reverse microemulsion method displayed a core-shell structure with ~ 50 nm thick amorphous SiO_2 shell. Figure 11.2 schematically shows the synthesis procedure of 8-hydroxyquinoline (8-HQ) encapsulated CP-SNCs from Fe_3O_4@mSiO_2. The fabricated CP-SNCs were successively

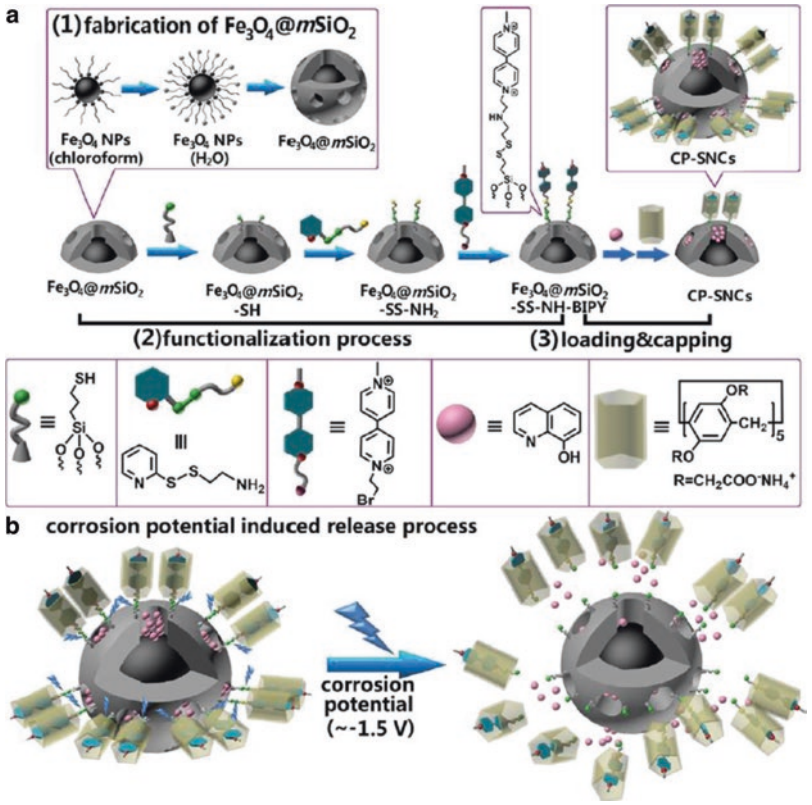

Fig. 11.2 Schematic diagrams of (**A**) Synthetic method of CP-SNCs [(1) Fabrication of Fe_3O_4@$mSiO_2$, (2) Functionalization process, and (3) Loading & Capping]; and (**B**) Corrosion potential-induced release. Reproduced with permission from Ref. 49; Copyright 2017 © American Chemical Society

assimilated into the hybrid sol-gel coating to construct CP-SFAC and coated on the AZ31B alloy [49]. The supramolecular assemblies with high binding affinity efficiently blocked the captured corrosion inhibitor (8-HQ), within the mesopores of Fe_3O_4@$mSiO_2$. At corrosion potentials (−1.5 V *vs* SHE, Mg alloy), the inhibitor gets released instantly because of the cleavage of disulfide linkers and the removal of the supramolecular assemblies (Fig. 11.2) [49].

An efficient inhibition strategy for early leakage through organosilyl modification at the outlet of mesopores were reported by Zheng et al. The nanocontainers assimilated coating showed good barrier effect, long-term self-healing and stimuli responsiveness to local pH change [50]. Zhao et al. fabricated hollow silica nanocapsules with $Mg(OH)_2$ precipitation in shells (HSNs) through an inverse emulsion polymerization where BTA has been immobilized in HSNs. Ultraviolet-visible (UV–vis) spectroscopic release studies at different pH values displayed that the amount of released BTA from the salt-precipitated HSNs in acidic solution was

considerably greater than that of HSNs without salt-precipitation [51]. Liang et al. reported an acid and alkali dual-stimuli responsive SiO_2-imidazoline nanocomposites (SiO_2–IMI) with high inhibitor loading capacity. The SiO_2-IMI were homogeneously disseminated into the hydrophobic SiO_2 sol, and a superhydrophobic surface was realized on Al alloy by dip-coating [52]. Wang et al. reported redox-triggered-smart-nanocontainers, assembled by mounting β CD functionalized with ferrocene onto the exterior surface of MSNs [53].

CDs are one of the foremost supramolecular hosts that can deliver diverse self-assembled structures and functionalities [17, 54, 55]. They are attractive in terms of availability, biocompatibility and cost factor. CDs are cyclic oligomers of glucose consisting of 6–8 D-glucopyranoside units connected edge to edge, with faces pointing inwards, headed for a central hydrophobic cavity wherein the interior cavity can accommodate guest molecules (Fig. 11.3). Amiri and Rahimi used α, β and γ forms of CD-based inclusion complex containing organic inhibitors to create on-demand release coatings. Salt spray test revealed that larger nanocontainer's size, higher nanocontainer content, and thicker coating afforded better corrosion protection. Corrosion initiation of the coated Al substrate happened after 6 days of salt spray on the bare sample, but the samples with nanocontainer-based coatings did not rust even after 1000 h [56, 57].

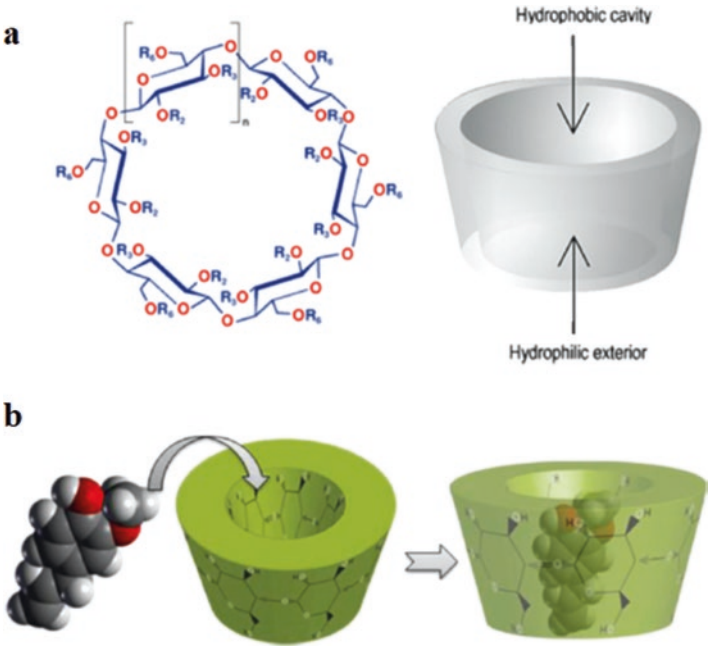

Fig. 11.3 (**a**) Molecular structure of CDs. (**b**) Schematic showing the formation of inclusion complex with guest molecule. Reproduced with permission from Ref. 56 & 57; Copyright 2015 & 2014 © Springer

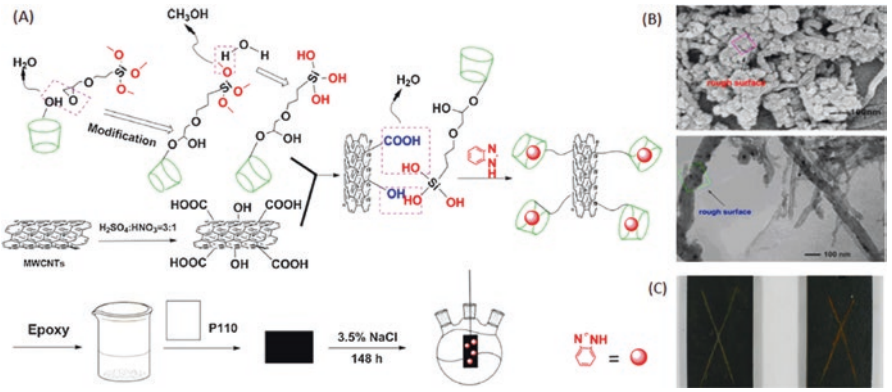

Fig. 11.4 (**A**) Synthesis of nanocontainers and fabrication sequence of the coating. (**B**) SEM and TEM images of MWCNTs/*β* CD. (**C**) Scarification test results (10 wt.% NaCl solution, 12 h) for steel specimens coated with (left) epoxy resin mixed with 3 wt.% *β* CD/MWCNTs loaded with inhibitor and (right) without corrosion inhibitor. Reproduced with permission from Ref. 58; Copyright 2016 © Elsevier

He et al. fabricated a nanoreservoir based on multi-walled carbon nanotubes (MWCNTs) and *β* CDs through a modest chemical way (Fig. 11.4). As evident from the SEM image, there was a noteworthy enlargement of MWCNTs after being amended by *β* CD, and that indicated that *β* CD was mounted on the surface of MWCNTs. TEM images (Fig. 11.4b) showed that it was an assembly of individual MWCNTs with heterogeneous layers. The *β* CD/MWCNTs were then loaded with a benzimidazole inhibitor and blended into epoxy. The scarification test in NaCl solution for 12 h (Fig. 11.4c) supported the better anti-corrosion and self-healing capability of the modified coating and that was ascribed to the controlled inhibitor release [58].

11.2.3 Inorganic Clay-Based

The inorganic clays have attracted much research attention as a low-cost nanocontainer. Halloysite clay nanotubes are the most widely investigated one. Halloysites appear in different morphologies, such as platy, spheroidal, and tubular, where the most prevalent morphology is tubular. The chemical formula of halloysite clay can be represented as $Al_2(OH)_4Si_2O_5{\cdot}nH_2O$. The hydrated halloysite (n = 2), called 'halloysite-10 (Å)', has a layer of water molecules between the adjacent clay layers (Fig. 11.5) [64].

The hollow structure of halloysite nanotubules can adequately encapsulate the active agent. The strong surface charges can permit multilayer-nanoscale-assemblies through LBL adsorptions, and that can be enclosed with polyelectrolytes to form

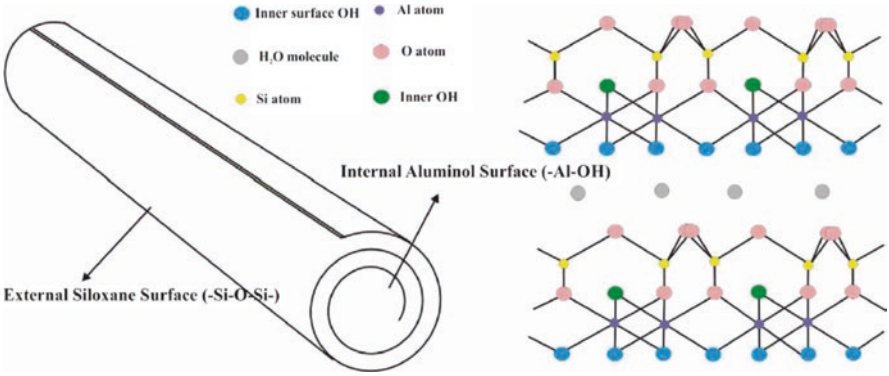

Fig. 11.5 Structure of halloysite clay particle. Reproduced with permission from Ref. 64; Copyright 2017 © Elsevier

nano-shells, overcrowding the tube ends and realizing controlled release of encapsulated inhibitors against an external stimulus [59]. Figure 11.6 shows scanning electron microscopy (SEM) images of halloysite nanotubes before and after loading a corrosion inhibitor (MBT). The initial halloysites comprise of well-defined nanotubes with sizes at the range of 1–15 μm. The maximum MBT quantity loaded was 5 wt.%. To achieve controlled release properties the nanotubes surfaces were modified by two polyelectrolyte bilayers [poly(styrene sulfonate) (PSS)/poly(allylamine hydrochloride) (PAH)] (Fig. 11.6) resulting in an inhibitor/halloysite/PAH/PSS/PAH/PSS layered structure. The opening of the shell can be realized by changing the system pH to acidic or alkali levels due to the onset of corrosion [22].

More details on inorganic clay nanocontainers can be found elsewhere [22, 60–64]. Several reports on anionic clays are available [65–67].

11.2.4 Polyelectrolyte-Based

Polyelectrolyte multilayers are widely investigated for smart coating applications. Polyelectrolytes (polymer + electrolyte) comprising of the fraction of monomeric units with ionized functional groups (cationic/anionic polyelectrolytes) can be assembled on the surface of nanoparticles via LBL approach. The incorporated inhibitors will be released in a controlled way when the confirmation of the polyelectrolyte molecules alters due to changes in pH or mechanical impact of the surrounding media [30, 68–71]. Polyelectrolytes can provide smart anti-corrosion protection due to different ways [70]:

- Buffering activity of the polyelectrolyte multilayers
- Self-curing due to mobility of the polyelectrolyte multilayers
- Polyelectrolyte multilayers as a carrier for corrosion inhibitors

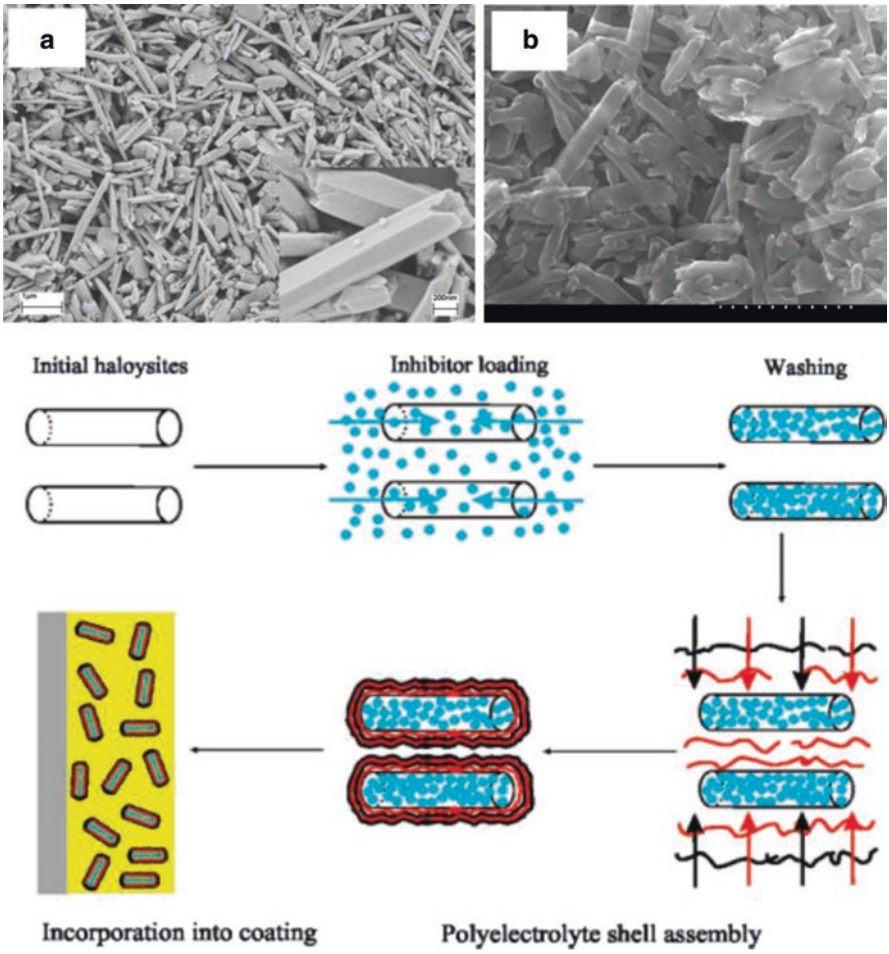

Fig. 11.6 SEM images of (**A**) as-formed halloysite nanotubes and (**B**) halloysites nanotubes doped with inhibitor (MBT) and coated with PAH/PSS/PAH/PSS polyelectrolyte layers (scale bar in B is 1.5 μm). Schematic illustration of the fabrication of MBT-loaded halloysite/polyelectrolyte nanocontainers is provided below. Reproduced with permission from Ref. 22; Copyright 2008 © American Chemical Society

A schematic showing the mechanism of action of smart self-healing polyelectrolyte coating with incorporated inhibitors is presented in Fig. 11.7. More details can be found elsewhere [68–71]

The design and preparation of novel supramolecular nanocontainers with multi-functionalities is anticipated to bring excellent prospects for developing new generation corrosion prevention coatings. In spite of the substantial extent of research efforts in this direction, there are only a few commercially offered products [27]. Many reported works available in the recent literature have the potential for industrial-scale applicability.

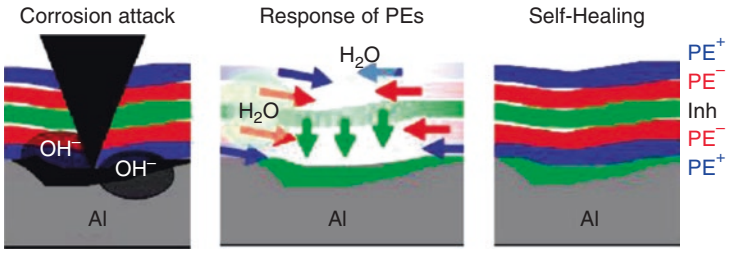

Fig. 11.7 Schematic mechanism of self-healing action of a smart polyelectrolyte anti-corrosion coating. Corrosion attack causes pH change of the system stimulating response of the polyelectrolyte coating: pH buffering, rearrangement of polymer chains and release of corrosion inhibitors (PE^+ – positively charged polyelectrolyte; PE^- – negatively charged polyelectrolyte; Inh – corrosion inhibitor). Reproduced with permission from Ref. 70; Copyright 2010 © American Chemical Society

11.3 Photoelectrochemical Cathodic Protection

Cathodic protection (sacrificial anode and impressed current methods) is an extensively employed corrosion prevention method. CP impedes corrosion by altering the active (anodic) sites on the metallic structure to passive (cathodic) sites by providing electrical current. The technique has a wide range of industrial applications; to mention a few, water/fuel pipelines, storing tanks, boat/ship hulls, offshore platforms, onshore well casings, and reinforcing steels. However, the cost factor occasionally limits the application.

While the sacrificial anode cathodic protection (SACP) works by the sacrificial current from an anode (e.g. Al, Mg); the impressed current (ICCP) method makes use of direct current from a rectifier to cathodically protect the steel. Both methods have advantages and disadvantages of their own. ICCP is not economic in terms of continuous usage of current whereas SACP is not attractive in terms of expensive anode materials. SACP is not considered environmentally friendly and the electrodes get consumed during the operation [72].

A recent environmentally friendly approach in this arena is photoelectrochemical cathodic protection (PECP) that utilizes renewable energy (solar energy) to generate electricity using a semiconductor photoelectrode (photoanode). On illumination, electrons in a semiconductor can be excited to conduction band yielding holes in valence band. The electrons produced can be used for protecting a metallic structure by altering the metal potential cathodically (to more negative values) than the potential at which corrosion occurs (Fig. 11.8). The photoanode does not get used up during the operation and is environmentally friendly. The method is economical as it does not consume electrical energy or waste anode material. The technique can be worthy for areas where power supplies are limited (Fig. 11.9).

TiO_2 is the extensively researched semiconducting transition metal oxide for photoanode fabrication. The material has attracted widespread research attention

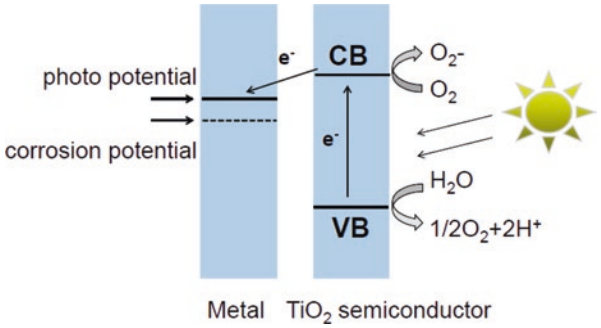

Fig. 11.8 The model of PECP of metal by semiconductor photoanode. Reproduced with permission from Ref. 73; Copyright 2017 © Creative Commons Licence

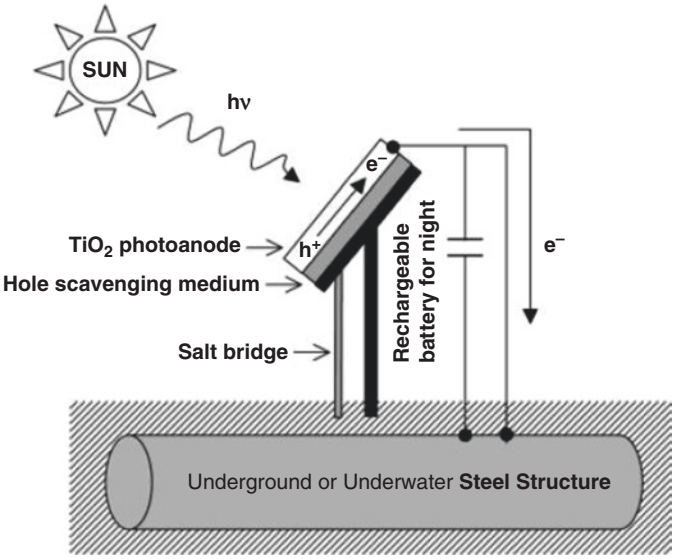

Fig. 11.9 Schematic diagram of the proposed photocathodic metal protection system using a TiO_2 photoanode and solar light. Reproduced with permission from Ref. 74; Copyright 2002 © American Chemical Society

because of its interesting photocatalytic properties, environmental friendliness, chemical stability and economic feasibility. The idea of PECP for metals by TiO_2 coatings under UV illumination was firstly reported in the year 1995 [75]. Since then, several studies have been reported on corrosion prevention of metals using TiO_2-based surface coatings [76, 77]. Park et al. further advanced the PECP technique motivated by the concept of employing a photoanode as an alternative to the sacrificial anode for prevention of steel corrosion. On UV illumination, a TiO_2 photoanode in contact with a hole scavenging medium can supply photocurrent to an electrically joined steel cathode, shifting the cathode potential to protective passive

values [74, 78]. Since then, PECP by TiO_2 photoanodes has received significant research attention [79–103]. In addition to the use of commercial TiO_2, different cost-effective approaches were employed for the preparation of TiO_2 such as sol-gel [79], hydrothermal [80], and liquid phase deposition [81]. Anodization of metallic Ti was also widely employed [82]. Among these methods, the liquid phase deposition (LPD) method is perhaps the most economical and can produce crystalline metal oxide semiconductor films at lower temperatures [81, 83, 84].

It is the wide bandgap (3.0 and 3.2 eV respectively for rutile and anatase phases) that limits photocatalytic properties of TiO_2 to UV region (wavelength < 390 nm). Different approaches were investigated to augment the photoactivity of TiO_2 from UV to the visible part, for example, metal/non-metal doping, dye sensitization, and semiconductor coupling. Among them, non-metal doping (with N, C, S etc.) [85, 86] has attracted significant recent research attention. It has been shown that N and F-doping eased the formation of surface oxygen vacancies, with a higher number of Ti^{3+} ions [85]. Sol-gel solvothermal synthesized N-F-doped TiO_2 presented excellent photocatalytic properties than a commercial-grade P25 TiO_2 [87]. Similarly, hydrothermally synthesized N-F-doped anatase TiO_2 from $(NH_4)_2TiF_6$ and NH_3 aqueous solutions showed strong absorption at 400–550 nm wavelength range [88]. Lei et al. have employed N-F-doped TiO_2 surface coating for the PECP of steel, that showed excellent visible light response at 600–750 nm wavelength range [81]. Although doping can reduce the band-gap, it has disadvantages such as indirect doping level with low absorption efficiency, and introduction of new recombination centers [73]. As an alternative to doping, semiconductor coupling was extensively researched.

Coupling TiO_2 with other semiconductors with appropriate energy levels is an accepted way to ease the separation of photoelectron-hole pairs. Small bandgap semiconductors, such as CdS [89], CdSe [90], PbS [91], PbSe [92] etc. have been introduced into mesoporous TiO_2 films to improve the visible light response. Zhang et al. reported a highly efficient CdSe/CdS co-sensitized TiO_2 nanotube films for PECP of stainless steel (SS) [93]. Li et al. reported an electrodeposited CdS-modified ordered anodized TiO_2 nanotubes photoelectrodes. The composite electrode efficiently harvested solar light in the UV and visible region and that was credited to the improved charge separation and electron transport efficiencies. The electrode potentials of 304 SS coupled with the composite photoanode shifted negatively for about 246 mV and 215 mV under UV and white light irradiation, respectively [94]. Several reports are available on carbon composite TiO_2 and polymer-modified TiO_2 photoanodes. More details can be found elsewhere [73].

Among the several alternatives reported for TiO_2, the graphitic carbon nitride (g-C_3N_4) is a recently reported promising material. However, the fast secondary recombination of photogenerated charge carriers and the amphoteric property of g-C_3N_4 are negatives. A nanocomposite with structured carbons, for example, graphene can improve the electrical conductivity and the charge separation efficiency of g-C_3N_4. Jing et al. reported a secondary reduced graphene oxide modified g-C_3N_4 (R-rGO-C_3N_4) that was prepared by a thermal polycondensation method and a subsequent reduction process (Fig. 11.10 A). An electrophoretic deposition was utilized

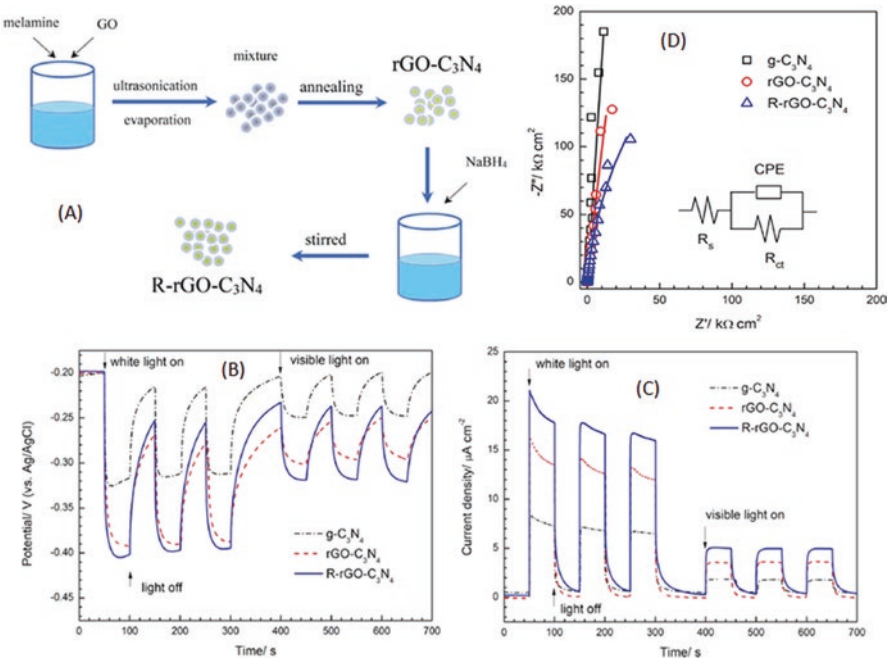

Fig. 11.10 (**A**) The schematic illustration of the preparation process of the R-rGO-C_3N_4 composite. The variations of the potentials (**B**) and current densities (**C**) of the 304 SS electrode coupled with the g-C_3N_4, rGO-C_3N_4 and R-rGO-C_3N_4 thin film photoanodes under intermittent light illumination. (**D**) Nyquist plots of the g-C_3N_4, rGO-C_3N_4 and R-rGO-C_3N_4 thin film photoanodes measured in the dark. The inset is the equivalent circuit used to fit the EIS results. Reproduced with permission from Ref. 95. Copyright 2017 © The Electrochemical Society

to fabricate the photoanode. The variations of the potentials and the current densities of the galvanic coupling under intermittent white light and visible light illumination are shown in Fig. 11.10 B & C. In dark, the potentials of all the three materials were close to the corrosion potential of 304 SS in 3.5 wt.% NaCl. The obvious shift of potential on light illumination corresponds to the cathodic polarization of steel. The photoinduced potential drops caused by rGO-C_3N_4 (190 mV) and R-rGO-C_3N_4 (200 mV) were larger than that of g-C_3N_4 (120 mV), demonstrating the better PECP performance of R-rGO-C_3N_4. The stability in potentials corresponds to stability of the prepared photoanodes. Positive current densities (Fig. 11.10 B) are detected for all the three galvanic couplings under light illumination, signifying successful electron transfer from the photoanode to the cathode. The photoinduced current densities of the g-C_3N_4, rGO-C_3N_4 and R-rGO-C_3N_4 photoanodes under white light illumination were approximately 7.4, 13.5 and 17.8 μA.cm^{-2}, respectively. Under visible light illumination, these values correspondingly decreased to 1.8, 3.5 and 5.1 μA.cm^{-2}. The charge transfer resistance (R_{ct}) was evaluated by performing electrochemical

impedance spectroscopy (EIS) studies in the dark at the open circuit potential (OCP) in 0.1 mol L^{-1} Na_2SO_4 (Fig. 11.10 D). The R_{ct} (obtained by curve fitting) of R-rGO-C_3N_4 (1.32×10^6 Ω.cm^2) was smaller than rGO-C_3N_4 (5.86×10^6 Ω.cm^2) and g-C_3N_4 (1.30×10^7 Ω.cm^2). The results displayed that rGO modification enhanced the electrical conductivity of g-C_3N_4, and promoted the transfer and separation of photogenerated charge carriers [95].

Another main issue in terms of commercialization of the technique is the absence of photoelectrochemical response of the photoanode in dark. In this direction, many research attempts are going on in fabricating novel photoanodes with extended energy (photoelectron) storage capacities in addition to PECP. The idea is to store surplus energy in the photoelectrode during day time so that it can be used at night. Several semiconductor transition metal oxides such as MoO_3 [96] and WO_3 [76, 97] were investigated along with TiO_2 in this direction. Bu and Ao classified the works reported in this domain as below:

- WO_3-TiO_2 composite photoanodes
- SnO_2-TiO_2 composite photoanodes
- CeO_2-TiO_2 composite photoanodes
- Porous structured TiO_2 photoanodes

Oxides of Mo and W are famous for their higher pseudocapacitance. Saji and Lee has investigated in detail the potential and pH-dependent pseudocapacitance of Mo-surface oxides [98–100]. A nanosized TiO_2/WO_3 bilayer coating on the surface of 304 SS was reported by Zho et al. and found that this coating could maintain the CP effect for 6 h in the dark after switching off the light [101]. Park et al. measured the galvanic current between the TiO_2/WO_3 photoelectrode and the coupled steel electrode and verified that the photoinduced electrons generated by TiO_2 transferred to WO_3 and then overflowed to the coupled steel during the light illumination, and the stored electrons in WO_3 flowed to the coupled steel directly or through TiO_2 after the light was switched off [102]. Liang et al. synthesized WO_3/TiO_2 nanotube composite film coated photoanodes where TiO_2 nanotubes were synthesized on Ti by electrochemical anodization, followed by annealing at 450 °C and WO_3 nanoparticles were deposited on the film via potentiostatic electrodeposition [97]. Other than coupling with semiconductor, TiO_2 films with special porous structures were also found to have certain electron storage properties [73].

Li et al. fabricated CdSe/RGO/TiO_2 photoanodes by electrochemical deposition (Fig. 11.11A). Under visible-light illumination, the OCP of the photoanode coupled with 304 SS shifted cathodically indicative of efficient PECP. The photocurrent of the composite electrode (Curve d, Fig. 11.11 b) is ~ 8 times greater than that of pure TiO_2 (Curve b). The enhanced performance was credited to its fast electron transfer, large surface area and ordered mesoporous structure. The composite photoanode provided satisfactory CP even in the dark (Fig. 11.11B). The potentiodynamic polarization curves (Fig. 11.11 C) clearly showed the better performance of the composite electrode. On illumination, the corrosion potential of both CdSe/TiO_2 and CdSe/RGO/TiO_2 electrodes exhibited a significant cathodic shift compared

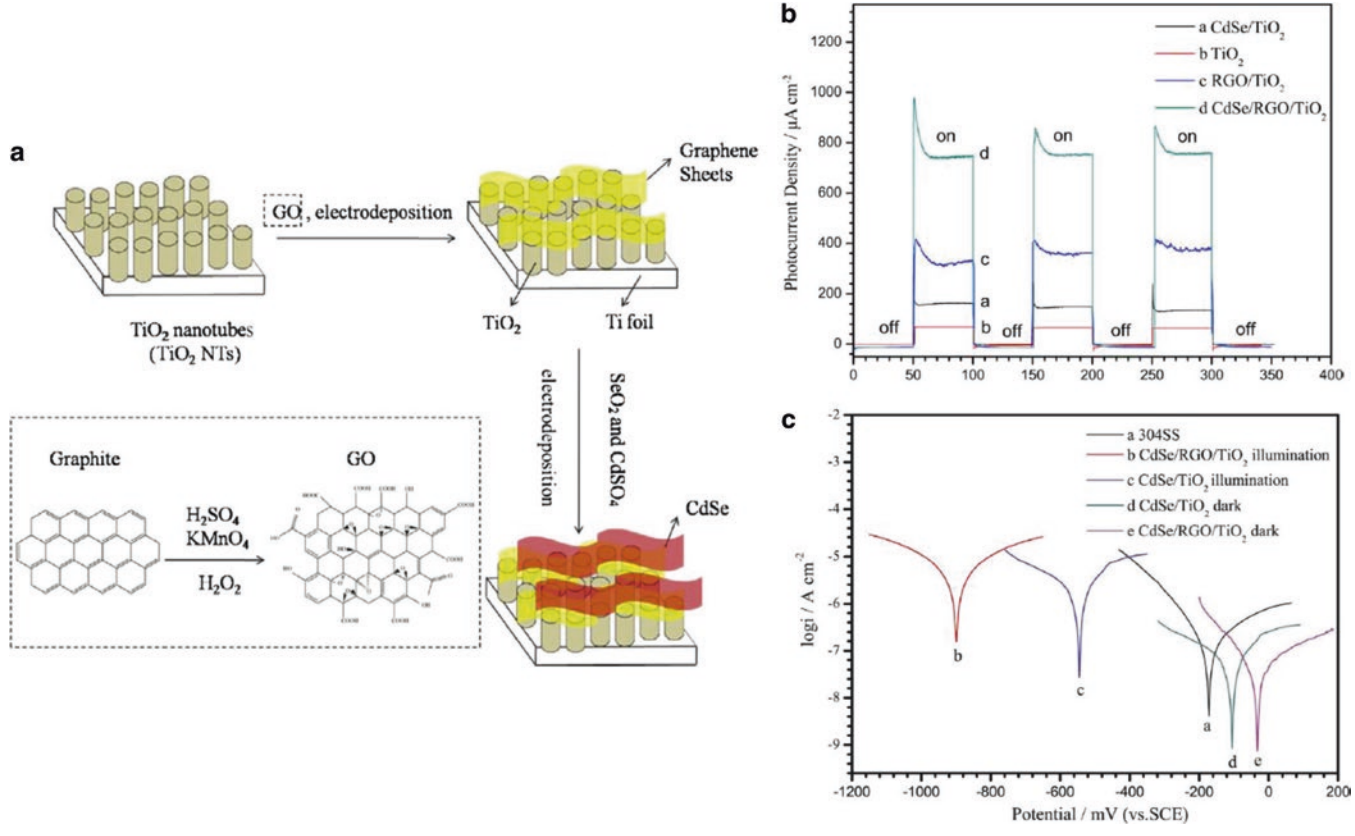

Fig. 11.11 (**A**) Schematic diagram of procedures for preparing the CdSe/RGO/TiO_2 composites. (**B**) Photocurrent-time curves of different photoanodes under intermittent illumination with visible light ($\lambda > 400$ nm). The electrolyte was 0.1 M Na_2SO_4 solution. The immersion time was 0.5 h. (**C**) Comparison of the polarization curves of bare 304 SS, and 304 SS coupled with CdSe/RGO/TiO_2 and CdSe/TiO_2 electrodes with or without visible-light illumination. The electrolyte in the corrosion cell was 3.5 wt.% NaCl solution, whereas in the photoanode cell was 0.1 M NaOH and 0.1 M Na_2S solution. Reproduced with permission from Ref. 103; Copyright 2015 @ Elsevier

with that of pure 304 SS in the dark. The corrosion potential shift was much more negative for CdSe/RGO/TiO_2 than CdSe/TiO_2 electrode. The corrosion current density exhibited a noteworthy increase when steel was coupled with CdSe/RGO/TiO_2 under illumination and that was attributed to the photogenerated electrons [103].

Table 11.1 shows a summary of PECP performance of TiO_2-based photoanodes [73]. Several works not presented in Table 11.1 are available in the current literature that includes Bi_2O_3/TiO_2 [104], g-C_3N_4/TiO_2 [105], $SrTiO_3/TiO_2$ [106], In_2O_3/TiO_2 [107], ZnO/In_2S_3 [108], NiO/TiO_2 [109], WO_3/TiO_2 [110], and RGO/WO_3/TiO_2 [111]. In spite of the fact the PECP technology has a high potential for industrial-scale application, more research efforts need to be put forward to enhance the protection efficiency and photoelectron storage capability.

Table 11.1 A summary of PECP performance of TiO_2-based photoanodes. Reproduced with permission from Ref. 73; Copyright 2017 © Creative Commons Licence

Photoanode	Method	Photo source	OCP (mV)	Metal
Pure TiO_2	Sol–gel	UV light	600	Cu
Pure TiO_2	Spray pyrolysis	UV light	250	304 SS
Pure TiO_2	LPD	White light	655	304 SS
Pure TiO_2	Anodization	White light	354	304 SS
Pure TiO_2	Hydro thermal	White light	262	316L SS
Pure TiO_2	Sol–gel	White light	525	304 SS
Pure TiO_2	Sol–gel	UV light	439	316L SS
Pure TiO_2	Sol–gel, hydrothermal	White light	560	403 SS
Ni–TiO_2	Sol–gel	Visible light	300	304 SS
Cr–TiO_2	Sol–gel	Simulated sunlight	230	316L SS
Fe–TiO_2	LPD	White light	405	304 SS
N–TiO_2	Anodization	Visible light	400	316L SS
N–TiO_2	Hydro thermal	UV light	470	316L SS
N–F–TiO_2	LPD	Visible light	515	304 SS
CdS/TiO_2	Anodization	UV light	246	304 SS
	Electrochemical deposition	White light	215	304 SS
ZnS/CdS@TiO_2	Anodization	White light	900	403 SS
	Electrochemical deposition			
Ag/SnO_2/TiO_2	Photo-reduction deposition, sol–gel	Visible light	550	304 SS
MWCNT/TiO_2	Sol–gel	UV light	400	304 SS
GR/TiO_2	Sol–gel	UV light	400	304 SS
Sodiumpolyacrylate/TiO_2	LPD	White light	710	304 SS

11.4 Conclusions and Outlook

The chapter provides a brief account of two promising corrosion prevention strategies that can be applied to desalination systems. In the first section, a short description of controlled on-demand release smart coatings with encapsulated inhibitors are provided. The section explains various nano/microcontainers that can be incorporated into the coating matrix for active protection. Among the four different types described, most of the recent works focused on mesoporous silica and cyclodextrin-based host-guest systems. Systematic practices need to be done in this area to optimize a particular nanocontainer in a coating, where the containers do not decline but augment the mechanical strength, adhesion and barrier properties of the coating. Further research is requisite in realizing sustained-release nanocontainers.

In the second section, the environmentally friendly solar energy-assisted cathodic protection, the photoelectrochemical cathodic protection is briefed. This concept is different from the photovoltaic powered cathodic protection (solar cells used as the external power source). Here, a semiconductor photoanode is utilized to generate electricity from solar light instead of using solar cell as a power source. These methods are worthy for areas where power supplies are limited. Non-metal doping of TiO_2 and semiconductor coupling of TiO_2 with charge storing transition metal oxides are highlighted in this section. In spite of having a few promising research, more works need to be performed in this area for its potential large scale application. Future research can be focused on combined systems of photoelectrochemical cathodic protection with traditional cathodic protection methods.

Acknowledgement The authors would like to acknowledge the support and fund provided by King Fahd University of Petroleum & Minerals through Project No. SR171021 under the Deanship of Research.

References

1. V.S. Saji, R. Cook, *Corrosion Control and Prevention Using Nanomaterials*, (Elsevier, 2012), ISBN 978-1-84569-949-9
2. G. Koch, J. Varney, N. Thompson, O. Moghissi, M. Gould, J. Payer, International measures of prevention, application, and economics of corrosion technologies study, *In* NACE International Impact, ed. by G. Jacobson, March 2016, Houston
3. L.T. Popoola, A.S. Grema, G.K. Latinwo, B. Gutti, A.S. Balogun, Corrosion problems during oil and gas production and its mitigation. Inter. J. Ind. Chem. **4**, 1–15 (2013)
4. M.G. Fontana, N.D. Greene, *Corrosion Engineering*, 3rd edn., (Mcgraw Hill, 1985), ISBN 978-0070214637
5. H.H. Uhlig, R.W. Review, (2009) *Corrosion and Corrosion Control: An Introduction to Corrosion Science and Engineering*, 4th edn., (Wiley, 2009), ISBN 978-0-471-73279-2
6. J. Kucera, Desalination – Water from Water, (Scrivener Publishing LLC, Massachusetts, Wiley, 2014), ISBN: 9781118208526
7. M. Elimelech, W.A. Phillip, The future of seawater desalination: Energy, technology, and the environment. Science **333**, 712–717 (2011)

8. A.E. Hughes, I.S. Cole, T.H. Muster, R.J. Varley, Designing green, self-healing coatings for metal protection. NPG Asia Mater. **2**, 143–151 (2010)
9. V.S. Saji, J. Thomas, Nano-materials for corrosion control. Corr. Sci. **92**, 51–55 (2007)
10. V.S. Raja, A. Venugopal, V.S. Saji, K. Sreekumar, S. Nair, M.C. Mittal, Electrochemical impedance behavior graphite dispersed electrically conducting acrylic coating on AZ 31 Mg alloy in 3.5 wt.% NaCl solution. Prog. Org. Coat. **67**, 12–19 (2010)
11. M. Jakab, J. Scully, On-demand release of corrosion-inhibiting ions from amorphous Al–co–Ce alloys. Nat. Mater. **4**, 667–670 (2005)
12. A.S.H. Makhlouf, *Handbook of Smart Coatings for Materials Protection*, (Elsevier, 2014), ISBN 9780857096883
13. S.V. Lamaka, M.L. Zheludkevich, K.A. Yasakau, R. Serra, S. Poznyak, M. Ferreira, Nanoporous titania interlayer as reservoir of corrosion inhibitors for coatings with self-healing ability. Prog. Org. Coat. **58**, 127–135 (2007)
14. Y. Feng, *Intelligent Nanocoatings for Corrosion Protection of Steels*, PhD Thesis, University of Calgary, (2017)
15. V.S. Saji, Supramolecular concepts and approaches in corrosion and biofouling prevention. Corr. Rev. **37**, 187–230 (2019)
16. J.M. Lehn, *Supramolecular Chemistry: Concepts and Perspectives*, (Wiley, 1995), ISBN 978-3527293117
17. J. Szejtli, T. Osa, *Comprehensive Supramolecular Chemistry*, Vol. 3, (Pergamon, 1999), ISBN 9780080912844
18. J.W. Steed, J.L. Atwood, *Supramolecular Chemistry*, (Wiley, 2000), ISBN 978-0-470-51234-0
19. J.M. Lehn, Towards complex matter: Supramolecular chemistry and self-organization. Proc. Natl. Acad. Sci. USA. **99**, 4763–4768 (2002)
20. J. Atwood, G.W. Gokel, L. Barbour, *Comprehensive Supramolecular Chemistry II*, 2nd edn., (Elsevier, 2017), ISBN 9780128031995
21. M.L. Zheludkevich, D.G. Shchukin, K.A. Yasakau, H. Möhwald, M.G.S. Ferreira, Anticorrosion coatings with self-healing effect based on nanocontainers impregnated with corrosion inhibitor. Chem. Mater. **19**, 402–411 (2007)
22. D.G. Shchukin, S.V. Lamaka, K.A. Yasakau, M.L. Zheludkevich, M.G.S. Ferreira, H. Möhwald, Active anticorrosion coatings with halloysite nanocontainers. J. Phys. Chem. C **112**, 958–964 (2008)
23. J. Baghdachi, Smart coatings, in *ACS Symposium Series*; (ACS, Washington, 2009), https://doi.org/10.1021/bk-2009-1002.ch001
24. M.L. Zheludkevich, J. Tedim, M.G.S. Ferreira, Smart coatings for active corrosion protection based on multi-functional micro and nanocontainers. Electrochim. Acta **82**, 314–323 (2012)
25. D.G. Shchukin, H. Möhwald, A coat of many functions. Science **341**, 1458–1459 (2013)
26. M.F. Montemor, Functional and smart coatings for corrosion protection: A review of recent advances. Surf. Coat. Technol. **258**, 17–37 (2014)
27. A. Stankiewicz, M.B. Barker, Development of self-healing coatings for corrosion protection on metallic structures. Smart Mater. Struct. **25**, 084013 (2016)
28. A.A. Nazeer, M. Madkour, Potential use of smart coatings for corrosion protection of metals and alloys: A review. J. Mol. Liq. **253**, 11–22 (2018)
29. F. Zhang, P. Ju, M. Pan, D. Zhang, Y. Huang, G. Li, X. Li, Self-healing mechanisms in smart protective coatings: A review. Corros. Sci. **144**, 74–88 (2018)
30. H. Wei, Y. Wang, J. Guo, N.Z. Shen, D. Jiang, X. Zhang, X. Yan, J. Zhu, Q. Wang, L. Shao, H. Lin, S. Wei, Z. Guo, Advanced micro/nanocapsules for self-healing smart anticorrosion coatings. J. Mater. Chem. A **3**, 469–480 (2015)
31. M. Huang, J. Yang, Facile microencapsulation of HDI for self-healing anticorrosion coatings. J. Mater. Chem. **21**, 11123–11130 (2011)
32. A. Latnikova, D.O. Grigoriev, H. Möhwald, D.G. Shchukin, Capsules made of cross-linked polymers and liquid core: Possible morphologies and their estimation on the basis of Hansen solubility parameters. J. Phys. Chem. **116**, 8181–8187 (2012)

33. V.V. Gite, P.D. Tatiya, R.J. Marathe, P.P. Mahulikar, D.G. Hundiwale, Microencapsulation of quinoline as a corrosion inhibitor in polyurea microcapsules for application in anticorrosive PU coatings. Prog. Org. Coat. **83**, 11–18 (2015)
34. G.L. Li, M. Schenderlein, Y. Men, H. Möhwald, D.G. Shchukin, Monodisperse polymeric core-shell nanocontainers for organic self-healing anticorrosion coatings. Adv. Mater. Interfaces **1**, 1300019 (2014)
35. F. Maia, K.A. Yasakau, J. Carneiro, S. Kallip, J. Tedim, T. Henriques, A. Cabral, J. Venâncio, M.L. Zheludkevich, M.G.S. Ferreira, Corrosion protection of AA2024 by sol-gel coatings modified with MBT-loaded polyurea microcapsules. Chem. Eng. J. **283**, 1108–1117 (2016)
36. A. Latnikova, D.O. Grigoriev, J. Hartmann, H. Möhwald, D.G. Shchukin, Polyfunctional active coatings with damage-triggered water-repelling effect. Soft Matter **7**, 369–372 (2011)
37. M. Cai, Y. Liang, F. Zhou, W. Liu, Functional ionic gels formed by supramolecular assembly of a novel low molecular weight anticorrosive/antioxidative gelator. J. Mater. Chem. **21**, 13399–13405 (2011)
38. V.C. Cécile, B. Fouzia, S. Pierre, J. Loïc, Surface-assisted self-assembly strategies leading to supramolecular hydrogels. Angew. Chem. Int. Ed. **57**, 1448–1456 (2018)
39. D.G. Shchukin, H. Möhwald, Self-repairing coatings containing active nanoreservoirs. Small **3**, 926–943 (2007)
40. A. Popoola, O.E. Olorunniwo, O.O. Ige, Corrosion resistance through the application of anti-corrosion coatings, in *Developments in Corrosion Protection*, (Intech, 2014). https://doi.org/10.5772/57420
41. B. Chang, J. Guo, C. Liu, J. Qian, W. Yang, Surface functionalization of magnetic mesoporous silica nanoparticles for controlled drug release. J. Mater. Chem. **20**, 9941–9947 (2010)
42. F. Maia, J. Tedim, A.D. Lisenkov, A.N. Salak, M.L. Zheludkevich, M.G.S. Ferreira, Silica nanocontainers for active corrosion protection. Nanoscale **4**, 1287–1298 (2012)
43. T.D. Nguyen, K.C.F. Leung, M. Liong, C.D. Pentecost, J.F. Stoddart, J.I. Zink, Construction of a pH-driven supramolecular nanovalve. Org. Lett. **8**, 3363–3366 (2006)
44. D. Borisova, H. Möhwald, D.G. Shchukin, Influence of embedded nanocontainers on the efficiency of active anticorrosive coatings for aluminum alloys part I: Influence of nanocontainer concentration. ACS Appl. Mater. Interfaces **4**, 2931–2939 (2012)
45. D. Borisova, H. Möhwald, D.G. Shchukin, Influence of embedded nanocontainers on the efficiency of active anticorrosive coatings for aluminum alloys part II: Influence of nanocontainer position. ACS Appl. Mater. Interfaces **5**, 80–87 (2013)
46. T. Chen, J.J. Fu, pH-responsive nanovalves based on hollow mesoporous silica spheres for controlled release of corrosion inhibitor. Nanotechnology **23**, 235605 (2012)
47. T. Chen, J.J. Fu, An intelligent anticorrosion coating based on pH-responsive supramolecular nanocontainers. Nanotechnology **23**, 505705 (2012)
48. C.D. Ding, Y. Liu, M.W. Wang, T. Wang, J.J. Fu, Self-healing, superhydrophobic coating based on mechanized silica nanoparticles for reliable protection of magnesium alloys. J. Mater. Chem. A **4**, 8041–8052 (2016)
49. C.D. Ding, J.H. Xu, L. Tong, G.C. Gong, W. Jiang, J. Fu, Design and fabrication of a novel stimulus-feedback anticorrosion coating featured by rapid self-healing functionality for the protection of magnesium alloy. ACS Appl. Mater. Interfaces **9**, 21034–21047 (2017)
50. Z. Zheng, M. Schenderlein, X. Huang, N.J. Brownbill, F. Blanc, D. Shchukin, Influence of functionalization of nanocontainers on self-healing anticorrosive coatings. ACS Appl. Mater. Interfaces **7**, 22756–22766 (2015)
51. D. Zhao, D. Liu, Z. Hu, A smart anticorrosion coating based on hollow silica nanocapsules with inorganic salt in shells. J. Coat. Technol. Res. **14**, 85–94 (2017)
52. Y. Liang, M.D. Wang, C. Wang, J. Feng, J.S. Li, L.J. Wang, J.J. Fu, Facile synthesis of smart nanocontainers as key components for construction of self-healing coating with superhydrophobic surfaces. Nanoscale Res. Lett. **11**, 231 (2016)
53. T. Wang, L.H. Tan, C.D. Ding, M.D. Wang, J.H. Xu, J.J. Fu, Redox-triggered controlled release systems-based bi-layered nanocomposite coating with synergistic self-healing property. J. Mater. Chem. A **5**, 1756–1768 (2017)

54. J. Szejtli, Introduction and general overview of cyclodextrin chemistry. Chem. Rev. **98**, 1743–1754 (1998)
55. W. Saenger, Cyclodextrin inclusion compounds in research and industry. Angew. Chem. Int. Ed. Engl. **19**, 344–362 (1980)
56. S. Amiri, A. Rahimi, Synthesis and characterization of supramolecular corrosion inhibitor nanocontainers for anticorrosion hybrid nanocomposite coatings. J. Polym. Res. **22**, 66 (2015)
57. S. Amiri, A. Rahimi, Preparation of supramolecular corrosion-inhibiting nanocontainers for self-protective hybrid nanocomposite coatings. J. Polym. Res. **21**, 566 (2014)
58. Y. He, C. Zhang, F. Wu, Z. Xu, Fabrication study of a new anticorrosion coating based on supramolecular nanocontainers. Synth. Met. **212**, 186–194 (2016)
59. E. Abdullayev, R. Price, D. Shchukin, Y. Lvov, Halloysite tubes as nanocontainers for anticorrosion coating with benzotriazole. ACS Appl. Mater. Interfaces **1**, 1437–1443 (2009)
60. D.G. Shchukin, H. Möhwald, Surface-engineered nanocontainers for entrapment of corrosion inhibitors. Adv. Funct. Mater. **17**, 1451–1458 (2007)
61. D. Fix, D.V. Andreeva, Y.M. Lvov, D.G. Shchukin, H. Möhwald, Application of inhibitor-loaded halloysite nanotubes in active anti-corrosive coatings. Adv. Funct. Mater. **19**, 1720–1727 (2009)
62. M.L. Zheludkevich, S.K. Poznyak, L.M. Rodrigues, D. Raps, T. Hack, L.F. Dick, T. Nunes, M.G.S. Ferreira, Active protection coatings with layered double hydroxide nanocontainers of corrosion inhibitor. Corros. Sci. **52**, 602–611 (2010)
63. J.M. Falcón, T. Sawczen, I.V. Aoki, Dodecylamine-loaded halloysite nanocontainers for active anticorrosion coatings. Front. Mater. **2**, 69 (2015)
64. K.A. Zahidah, S. Kakooei, M.C. Ismail, P.B. Raja, Halloysite nanotubes as nanocontainer for smart coating application: A review. Prog. Org. Coat. **111**, 175–185 (2017)
65. D. Álvarez, A. Collazo, M. Hernández, X.R. Nóvoa, C. Pérez, Characterization of hybrid sol-gel coatings doped with hydrotalcite-like compounds to improve corrosion resistance of AA2024-T3 alloys. Prog. Org. Coat. **67**, 152–160 (2010)
66. N.C. Rosero-Navarro, L. Paussa, F. Andreatta, Y. Castro, A. Durán, M. Aparicio, L. Fedrizzi, Optimization of hybrid sol-gel coatings by combination of layers with complementary properties for corrosion protection of AA2024. Prog. Org. Coat. **69**, 167–174 (2010)
67. J. Tedim, S.K. Poznyak, A. Kuznetsova, D. Raps, T. Hack, M.L. Zheludkevich, M.G.S. Ferreira, Enhancement of active corrosion protection via combination of inhibitor-loaded nanocontainers. ACS Appl. Mater. Interfaces **2**, 1528–1535 (2010)
68. I. Dewald, A. Fery, Polymeric micelles and vesicles in polyelectrolyte multilayers: Introducing hierarchy and compartmentalization. Adv. Mater. Interfaces **4**, 1600317 (2017)
69. D.O. Grigoriev, K. Köhler, E. Skorb, D.G. Shchukin, H. Möhwald, Polyelectrolyte complexes as a smart depot for self-healing anticorrosion coatings. Soft Matter **5**, 1426–1432 (2009)
70. D.V. Andreeva, E.V. Skorb, D.G. Shchukin, Layer-by-layer polyelectrolyte/inhibitor nanostructures for metal corrosion protection. ACS Appl. Mater. Interfaces **2**, 1954–1962 (2010)
71. M. Biesalski, J. Ruehe, R. Kuegler, W. Knoll, Polyelectrolytes at solid surfaces: Multilayers and brushes, *In Handbook of Polyelectrolytes and their Applications*, ed. by S.K. Tripathy, J. Kumar, H.S. Nalwa, Vol. 1, (2002), 39–63
72. W. von Baeckmann, W. Schwenk, W. Prinz, *Handbook of Cathodic Corrosion Protection*, 3rd edn., ISBN: 9780884150565, (Elsevier, 1997)
73. Y. Bu, J.P. Ao, A review on photoelectrochemical cathodic protection semiconductor thin films for metals. Green Energy Environ. **2**, 331–362 (2014)
74. H. Park, K.Y. Kim, W. Choi, Photoelectrochemical approach for metal corrosion prevention using a semiconductor photoanode. J. Phys. Chem. B **106**, 4775–4781 (2002)
75. J. Yuan, S. Tsujikawa, Characterization of sol-gel-derived TiO_2 coatings and their photoeffects on copper substrates. J. Electrochem. Soc. **142**, 3444–3450 (1995)
76. T. Tatsuma, S. Saitoh, Y. Ohko, A. Fujishima, TiO_2-WO_3 photoelectrochemical anticorrosion system with an energy storage ability. Chem. Mater. **13**, 2838–2842 (2001)

77. Y. Ohko, S. Saitoh, T. Tatsuma, Fujishima, A Photoelectrochemical anticorrosion and self-cleaning effects of a TiO_2 coating for type 304 stainless steel. J. Electrochem. Soc **148**, B24–B28 (2001)
78. H. Park, K.Y. Kim, W. Choi, A novel photoelectrochemical method of metal corrosion prevention using a TiO_2 solar panel. Chem. Commun., 281–282 (2001)
79. R. Subasri, T. Shinohara, Investigations on SnO_2-TiO_2 composite photoelectrodes for corrosion protection. Electrochem. Commun. **5**, 897–902 (2003)
80. Y.F. Zhu, R.G. Du, W. Chen, H.Q. Qi, C.J. Lin, Photocathodic protection properties of three-dimensional titanate nanowire network films prepared by a combined sol–gel and hydrothermal method. Electrochem. Commun. **12**, 1626–1629 (2010)
81. C.X. Lei, Z.D. Feng, H. Zho, Visible-light-driven photogenerated cathodic protection of stainless steel by liquid-phase-deposited TiO_2 films. Electrochim. Acta **68**, 134–140 (2012)
82. J. Li, C.J. Lin, C.G. Lin, A photoelectrochemical study of highly ordered TiO_2 nanotube arrays as the photoanodes for cathodic protection of 304 stainless steel. J. Electrochem. Soc. **158**, C55–C62 (2011)
83. C.X. Lei, H. Zhou, Z.D. Feng, Effect of liquid-phase-deposited parameters on the photogenerated cathodic protection properties of TiO_2 films. J. Alloys Compd **542**, 164–169 (2012)
84. T.P. Niesen, M.R. De Guire, Review: Deposition of ceramic thin films at low temperatures from aqueous solutions. J. Electroceram. **6**, 169–207 (2001)
85. D. Li, N. Ohashi, S. Hishita, T. Kolodiazhnyi, H. Haneda, Origin of visible-light-driven photocatalysis: A comparative study on N/F-doped and N–F-codoped TiO_2 powders by means of experimental characterizations and theoretical calculations. J. Solid State Chem. **178**, 3293–3302 (2005)
86. H. Yun, J. Li, H.B. Chen, C.J. Lin, A study on the N-, S- and Cl-modified nano-TiO_2 coatings for corrosion protection of stainless steel. Electrochim. Acta **52**, 6679–6685 (2007)
87. D.G. Huang, S.J. Liao, J.M. Liu, Z. Dang, L. Petrik, Preparation of visible-light responsive N-F-codoped TiO_2 photocatalyst by a sol–gel-solvothermal method. J. Photochem. Photobiol. A Chem. **184**, 282–288 (2006)
88. T. Yamada, Y. Gao, M. Nagai, Hydrothermal synthesis and evaluation of visible light active photocatalysts of (N, F)-codoped anatase TiO_2 from an F-containing titanium chemical. J. Ceram. Soc. Jpn. **116**, 614–618 (2008)
89. B. Jiang, X.L. Yang, X. Li, D.Q. Zhang, J. Zhu, G.S. Li, Core–shell structure CdS/TiO_2 for enhanced visible-light-driven photocatalytic organic pollutants degradation. J. Sol-Gel Sci. Technol. **66**, 504–511 (2013)
90. L.L. Su, J. Lv, H.E. Wang, L.J. Liu, G.Q. Xu, D.M. Wang, Z.X. Zheng, Y.C. Wu, Improved visible light photocatalytic activity of CdSe modified TiO_2 nanotube arrays with different intertube spaces. Catal. Lett. **144**, 553–560 (2014)
91. R. Plass, S. Pelet, J. Krueger, M. Gratzel, U. Bach, Quantum dot sensitization of organic–inorganic hybrid solar cells. J. Phys. Chem. B **106**(2002), 7578–7580 (2002)
92. R.D. Schaller, V.I. Klimov, High efficiency carrier multiplication in PbSe nanocrystals: Implications for solar energy conversion. Phys. Rev. Lett. **92**, 186601 (2004)
93. J. Zhang, R.G. Du, Z.Q. Lin, Y.F. Zhu, Y. Guo, H.Q. Qi, L. Xu, C.J. Lin, Highly efficient CdSe/CdS co-sensitized TiO_2 nanotube films for photocathodic protection of stainless steel. Electrochim. Acta **83**, 59–64 (2012)
94. J. Li, C.J. Lin, J.T. Li, Z.Q. Lin, A photoelectrochemical study of CdS modified TiO_2 nanotube arrays as photoanodes for cathodic protection of stainless steel. Thin Solid Films **519**, 5494–5502 (2011)
95. J. Jing, M. Sun, Z. Chen, J. Li, F. Xu, L. Xu, Enhanced photoelectrochemical cathodic protection performance of the secondary reduced graphene oxide modified graphitic carbon nitride. J. Electrochem. Soc. **164**, C822–C830 (2017)
96. Q. Liu, J. Hu, Y. Liang, Z.C. Guan, H. Zhang, H.P. Wang, R.G. Du, Preparation of MoO_3/TiO_2 composite films and their application in photoelectrochemical anticorrosion. J. Electrochem. Soc. **163**, C539–C544 (2016)

97. Y. Liang, Z.C. Guan, H.P. Wang, R.G. Du, Enhanced photoelectrochemical anticorrosion performance of WO_3/TiO_2 nanotube composite films formed by anodization and electrodeposition. Electrochem. Commun. **77**, 120–123 (2017)
98. V.S. Saji, C.W. Lee, Molybdenum, molybdenum oxides and their electrochemistry. ChemSusChem **5**, 1146–1161 (2012)
99. V.S. Saji, C.W. Lee, Reversible redox transition and pseudocapacitance of molybdenum/surface molybdenum oxides. J. Electrochem. Soc. **160**, H54–H61 (2013)
100. V.S. Saji, C.W. Lee, Potential and pH-dependent pseudocapacitance of Mo/Mo oxides – An impedance study. Electrochim. Acta **137**, 647–653 (2014)
101. M. Zhou, Z. Zeng, L. Zhong, Photogenerated cathode protection properties of nano-sized TiO_2/WO_3 coating. Corros. Sci. **51**, 1386–1391 (2009)
102. H. Park, A. Bak, T. Jeon, S. Kim, W. Choi, Photo-chargeable and dischargeable TiO_2 and WO3 heterojunction electrodes. Appl. Catal. B Environ. **115-116**, 74–80 (2012)
103. H. Li, X. Wang, L. Zhang, B. Hou, Preparation and photocathodic protection performance of CdSe/reduced graphene oxide/TiO_2 composite. Corros. Sci. **94**, 342–349 (2015)
104. Z.-C. Guan, H.-P. Wang, X. Wang, J. Hu, R.-G. Du, Fabrication of heterostructured β-Bi2O3-TiO2 nanotube array composite film for photoelectrochemical cathodic protection applications. Corros. Sci. **136**, 60–69 (2018)
105. D. Ding, Q. Hou, Y. Su, Q. Li, L. Liu, J. Jing, B. Lin, Y. Chen, g-C3N4/TiO2 hybrid film on the metal surface, a cheap and efficient sunlight active photoelectrochemical anticorrosion coating. J. Mater. Sci. Mater. Electron. **30**, 12710–12717 (2019)
106. Y.-F. Zhu, L. Xu, J. Hu, J. Zhang, R.-G. Du, C.-J. Lin, Fabrication of heterostructured SrTiO3/TiO2 nanotube array films and their use in photocathodic protection of stainless steel. Electrochim. Acta **121**, 361–368 (2014)
107. M. Sun, Z. Chen, Enhanced photoelectrochemical cathodic protection performance of the in O/TiO composite. J. Electrochem. Soc. **162**, C96–C104 (2014)
108. J. Jing, Z. Chen, Y. Bu, Visible light induced photoelectrochemical cathodic protection for 304 SS by In2S3-sensitized ZnO nanorod array. Int. J. Electrochem. Sci. **10**, 8783–8796 (2015)
109. C. Han, Q. Shao, J. Lei, Y. Zhu, S. Ge, Preparation of NiO/TiO2 p-n heterojunction composites and its photocathodic protection properties for 304 stainless steel under simulated solar light. J. Alloys Compd. **703**, 530–537 (2017)
110. S.Q. Yu, Y.H. Ling, R.G. Wang, J. Zhang, F. Qin, Z.J. Zhang, Constructing superhydrophobic WO3@TiO2 nanoflake surface beyond amorphous alloy against electrochemical corrosion on iron steel. Appl. Surf. Sci. **436**, 527–535 (2018)
111. W. Liu, T. Du, Q. Ru, S. Zuo, Y. Cai, C. Yao, Preparation of graphene/WO3/TiO2 composite and its photocathodic protection performance for 304 stainless steel. Mater. Res. Bull. **102**, 399–405 (2018)